External feedback control of chaos using approximate periodic orbits

Kazuyuki Yagasaki and Moriyoshi Kumagai*
Department of Mechanical and Systems Engineering, Gifu University, Gifu, Gifu 501-1193, Japan
(Received 26 March 2001; revised manuscript received 13 August 2001; published 11 January 2002)

We apply the external feedback technique to control chaos in real physical systems. The target, unstable periodic orbits embedded in chaotic attractors are obtained from chaotic time series in terms of the delay coordinates technique. We demonstrate its efficiency for periodically forced, single- and two-degree-of-freedom systems consisting of one or two pendula in numerical simulations and experiments.

DOI: 10.1103/PhysRevE.65.026204 PACS number(s): 05.45.Gg, 07.05.Dz, 45.80.+r

I. INTRODUCTION

Chaos control has attracted much attention in the past decade and some techniques for controlling chaotic dynamical systems have been developed [1,2]. Among them, Pyragas [3] proposed two effective control methods for continuous chaotic dynamical systems. Consider a situation in which the governing equation is given by

$$\dot{\xi}=P(\xi,\eta), \quad \dot{\eta}=Q(\xi,\eta)+F(t), \tag{1}$$

where $\xi\in\mathbb{R}^{n-1}$ is not available or not of interest, only $\eta\in\mathbb{R}$ can be measured, P: $\mathbb{R}^{n-1}\times\mathbb{R}\to\mathbb{R}^{n-1}$ and Q:$\mathbb{R}^{n-1}\times\mathbb{R}\to\mathbb{R}$ are sufficiently smooth, and $F(t)$ is the control force, and assume that Eqs. (1) have a chaotic attractor when $F=0$. In this setting, he proposed two types of feedback control, *external feedback control*

$$F(t)=\kappa(\overline{\eta}(t)-\eta) \tag{2}$$

and *delayed feedback control*

$$F(t)=\kappa(\eta(t-\tau)-\eta(t)), \tag{3}$$

to stabilize an unstable periodic orbit (UPO) embedded in the chaotic attractor. Here $\overline{\eta}(t)$ is the UPO to be stabilized and τ is its period. In particular, the delayed feedback control technique has been applied experimentally to many mechanical, electric, chemical, and biological problems [2,4], and it was also extended to improve its efficiency [5]. However, it was shown numerically [6] (see also Sec. III) and theoretically [7] that the effectiveness of the method is very restrictive.

On the other hand, the external feedback control was actually used to control chaos in only very limited cases. To the authors' knowledge, there has been no experimental application except Ref. [8], in which *a priori* given equilibrium states were stabilized in an electric circuit. So it is still unknown whether this method is valid or not for stabilizing UPOs embedded in chaotic attractors. Especially, obtaining precise UPOs enough for chaos control seems difficult although a rough idea to overcome the problem was stated in Pyragas' original paper [3]. It should also be noted that providing large perturbations (e.g., the use of large feedback gain and an attempt to stabilize the periodic orbit existing for different parameter values) to systems as in Sec. 4 of [9] is inappropriate in some applications.

In this paper, we apply the external feedback technique to control chaos in real physical systems. The target UPOs are obtained from chaotic time series in terms of the delay coordinates technique [10,11], basically according to Pyragas' rough idea. We demonstrate its efficiency for periodically forced, single-, and two-degree-of-freedom systems consisting of one or two pendula in numerical simulations and experiments.

The outline of this paper is as follows. In Sec. II our external feedback control technique is described. In particular, an approach to obtain the target UPOs from chaotic time series based on the delay coordinates technique is presented. Numerical simulation and experimental results for periodically forced, single, and coupled pendula are given in Secs. III and IV. Finally, a summary and some comments are stated in Sec. V.

II. APPROACH

Consider systems of the form [12]

$$\dot{x}=f(x,t), \quad y=g(x), \quad x\in\mathbb{R}^n, \quad y\in\mathbb{R}^m, \tag{4}$$

where f:$\mathbb{R}^n\times\mathbb{R}\to\mathbb{R}^n$ ($n\geqslant 2$) and g:$\mathbb{R}^n\to\mathbb{R}^m$ ($m\geqslant 1$) are sufficiently smooth, and f is τ-periodic in t. Here x denotes the state of the system and y the output. So only y can be measured. Equations (4) are assumed to exhibit chaotic motions. Note that any periodic orbit in Eqs. (4) has a period of the form $k\tau$ with k some positive integer. In the following, we only treat the case of τ-periodic orbits, although an extension of the result to $k\tau$-periodic orbits is obvious.

Let $\overline{x}(t)$ be an unstable τ-periodic orbit near the chaotic attractor in the first equation of Eqs. (4), and let $\overline{y}(t)$ be the corresponding τ-periodic output, i.e., $\overline{y}(t)=g(\overline{x}(t))$. We attempt to stabilize the orbit $\overline{y}(t)$ by external feedback, so that the governing equation becomes

$$\dot{x}=f(x,t)+K[\overline{y}(t)-y] \quad [y=g(x)], \tag{5}$$

where K is an $n\times m$ matrix. Equation (5) contains Pyragas' case of Eqs. (1) with external feedback as a special one. In realistic situations, the exact UPO $\overline{y}(t)$ is difficult to obtain since it is unobservable. However, when the system (4) exhibits chaos, one can sometimes obtain an approximation for $\overline{y}(t)$ from chaotic time series of $y(t)$, e.g., using a method of Lathrop and Kostelich [11], as described below. If such an

*Present address: Meikikou Corporation, 180 Higashi, Okute-cho, Toyoake, Aichi 470-1111, Japan.

 ©2002 The American Physical Society

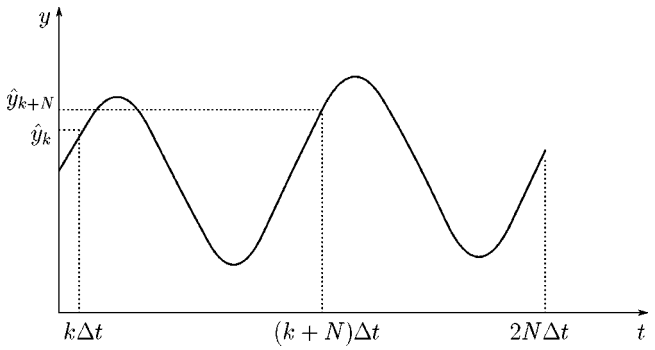

FIG. 1. Determination of an approximate UPO. Here the time t is reset at $t=j'\tau$.

approximate UPO $\overline{y}(t)$ is obtained, then we use it instead of the exact UPO, so that Eq. (5) is changed as

$$\dot{x}=f(x,t)+K[\tilde{y}(t)-y]. \tag{6}$$

We now describe an approach to obtain an approximate UPO $\tilde{y}(t)$. For simplicity, we assume that the observable variable y is scalar, i.e., $y\in\mathbb{R}$, and two-dimensional delay coordinates [10] $(y(i\tau),y[(i+1)\tau])$, $i=1,2,3,\ldots$, are used. An extension of the approach to higher-dimensional cases is obvious.

We first sample a chaotic time series of $y(t)$ at $t=\tau,2\tau,3\tau,\ldots$. Denote by y_i, $i=1,2,3,\ldots$, this time series. Using a technique of [11], we can detect an approximate locus of a UPO at $t=0$: if

$$\max(|y_{j+2}-y_{j+1}|,|y_{j+1}-y_j|)<r_0 \tag{7}$$

for some integer $j>0$ and some small constant $r_0>0$, then there exists a τ-periodic orbit $\overline{y}(t)$ such that $\overline{y}(i\tau)\approx y_{j+1}$ for $i=0,\pm1,\ldots$. Let $\tilde{y}_0$ be one of such points corresponding to approximate UPOs.

We next sample another chaotic time series of $y(t)$ and denote it by y'_i, $i=1,2,3,\ldots$. Suppose that we find successive points $y'_{j'+i}$, $i=0,1,2$, in the time series such that condition (7) holds as $y_{j+i}=y'_{j'+i}$, $i=0,1,2$, i.e.,

$$\max(|y'_{j'+2}-y'_{j'+1}|,|y'_{j'+1}-y'_{j'}|)<r_0 \tag{8}$$

and

$$\max(|y'_j-\tilde{y}_0|,|y'_{j+1}-\tilde{y}_0|,|y'_{j+2}-\tilde{y}_0|)<r_1, \tag{9}$$

where $r_1>0$ is a small constant. Then we record $y(t)$ at a short interval Δt for $j'\tau\leqslant t\leqslant(j'+2)\tau$, where $N\Delta t=\tau$ for some large integer $N>0$. Let $\hat{y}_i=y(j'\tau+i\Delta t)$, $i=0,1,\ldots,2N$, be the recorded data corresponding to a wave form of $y(t)$ with length 2τ. In particular, $\hat{y}_0=y'_{j'}$, $\hat{y}_N=y'_{j'+1}$, and $\hat{y}_{2N}=y'_{j'+2}$.

Finally, using the recorded data $\hat{y}_i$, $i=0,\ldots,2N$, we search for an integer $k>0$ such that

$$|\hat{y}_{k+N}-\hat{y}_k|=\text{minimum} \tag{10}$$

(see Fig. 1) and take

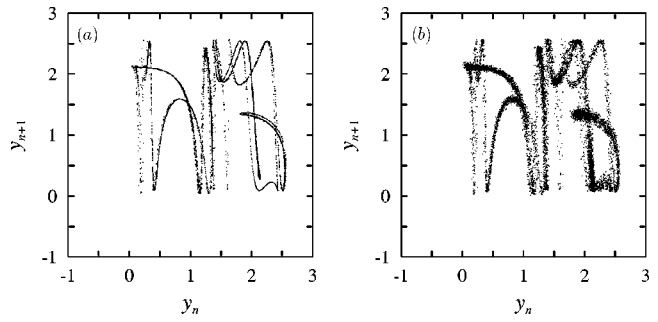

FIG. 2. Numerically computed chaotic attractors in Eqs. (14) with $\delta=0.5$, $\gamma=1.6$, and $\omega=\pi/5$: (a) $\sigma=0$; (b) $\sigma=0.03$. Here σ represents the intensity of the added Gaussian white noise.

$$\tilde{y}(t)=\begin{cases}\hat{y}_{i+N} & \text{if } 0\leqslant i<k,\\ \hat{y}_i & \text{if } k\leqslant i\leqslant N\end{cases} \tag{11}$$

for $t\in[i\Delta t,(i+1)\Delta t)$ as an approximate UPO corresponding to the point $\tilde{y}_0$ obtained from the first time series. The memory this approach requires is not so large.

We can also use the approach of [13] to keep the control force

$$u=K[\tilde{y}(t)-y] \tag{12}$$

small if it is applied for $t\in[i\tau,(i+1)\tau)$ only when

$$\max(|y[(i-1)\tau]-\tilde{y}(0)|,|y(i\tau)-\tilde{y}(0)|)<r_2 \tag{13}$$

for some small constant $r_2>0$. In addition, this treatment prevents the birth of undesirable stable orbits by the external feedback control.

In the following sections, we give numerical and experimental results for periodically forced, single and coupled pendula to demonstrate the effectiveness of this chaos control technique.

III. NUMERICAL SIMULATIONS FOR A FORCED PENDULUM WITH LINEAR DAMPING

The first example is a periodically forced pendulum with linear damping, for which the dimensionless governing equation is given by

$$\dot{x}_1=x_2,\quad \dot{x}_2=-\sin x_1-\delta x_2+\gamma\cos\omega t, \tag{14}$$

where δ, γ, and ω are positive constants and the period is $\tau=2\pi/\omega$. Only the velocity $y=x_2$ is assumed to be measured. We fix the parameter values as $\delta=0.5$, $\gamma=1.6$, and $\omega=\pi/5$, which were also chosen in [6].

Figure 2 shows numerically computed chaotic attractors[1] in the delay coordinates (y_n,y_{n+1}). The attractors are obviously folded so that an extra dimension is required to recon-

[1]Using computer software called DYNAMICS [14], we computed the Lyapunov exponents for Eqs. (14). The obtained maximum Lyapunov exponent is approximately 0.110 and chaotic motions occur in Eqs. (14).

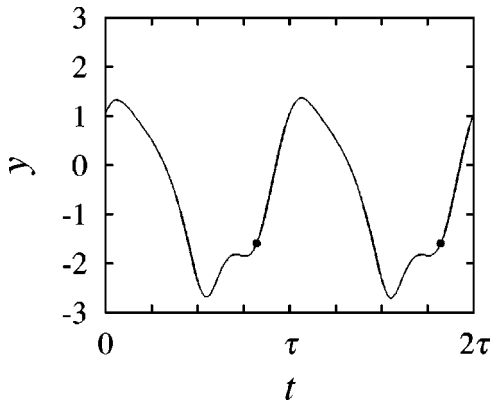

FIG. 3. Approximate UPO detected in numerical simulations of Eqs. (14) for $\delta=0.5$, $\gamma=1.6$, and $\omega=\pi/5$. The dots represent an edge of the UPO.

struct them globally [15]. However, the information we need is local, and two-dimensional coordinates are enough for our purpose (see the Appendix). In Fig. 2(b), a Gaussian white noise with mean zero and intensity $\sigma=0.03$ is added on the right-hand side of the second equation of Eqs. (14). Such an influence of noise must be taken into consideration for application to real physical systems. In both Figs. 2(a) and 2(b), 10 000 data after 100 periods under the initial condition $x_1=x_2=0$ are plotted.

The approach of Sec. II with $r_0=0.05$ and $r_1=0.1$ was used to obtain an approximate τ-periodic orbit $\tilde{y}(t)$ when the Gaussian white noise of $\sigma=0.03$ was added. The time series of y given in Fig. 2(b) was used to detect the approximate locus of the UPO, which was estimated as $\tilde{y}_0\approx 1.044$. The second time series of y was calculated under the initial condition $x_1=1$ and $x_2=0$ for another sample of the white noise. Figure 3 shows the obtained approximate UPO. Using the approach, we could also obtain a symmetric counterpart for Fig. 3 but could not obtain other UPOs from these time series.

To stabilize the UPO of Fig. 3, we apply the external feedback control so that control force $u=\kappa(\tilde{y}(t)-y)$ was added to the second equation of Eqs. (14). Using computer software called AUTO [16] with a driver called HomMap [17], we computed the stability boundaries for a numerically computed UPO corresponding to the approximate UPO of Fig. 3. The result is shown in Fig. 4. The stability boundaries for the same UPO when the delayed feedback control $\kappa[y(t-\tau)-y(t)]$ is applied instead of the external feedback control are also drawn in Fig. 4. Here the stability regions for the delayed feedback control were numerically obtained using the linear stability theory of time-delay differential equations [18] as in [6,19]. We see that the stability region for the external feedback control is much larger than that for the delayed feedback control. Smallness of the stability region when the delayed feedback control and its extensions are applied to a different periodic orbit was also observed in [6]. We also remark that large external feedback gain can always stabilize the target in Fig. 4, but this is not the case when an approximate UPO is used since the perturbation applied to the system is so large that there can exist no periodic orbit near the UPO.

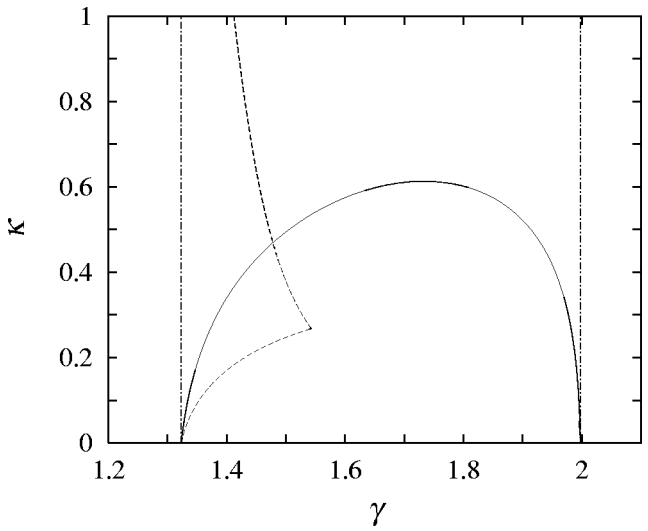

FIG. 4. Stability boundaries of a UPO corresponding to the approximate UPO in Fig. 3. The solid curve represents the stability boundary for the UPO when the external feedback control is applied. Above the curve the UPO becomes stable. The broken and dash-dotted curves, respectively, represent the stability boundaries when the delayed feedback control and no control are applied. A very small stability region for the delayed feedback control exists near $(\gamma,\kappa)=(2,0)$, although it is almost invisible.

We tried to stabilize the UPO from $n=0$ to $n=1500$ and applied no feedback control force after $n=1500$, where n represents time with the period of the external force as a unit. The approach stated at the end of Sec. II was also used to keep the control force small. Figure 5 shows the result for $\kappa=0.6$ and $r_2=0.2$. Time series of the dimensionless velocity y and external feedback control force u sampled at $\omega t=0 \bmod 2\pi$ are drawn in Figs. 5(a) and 5(b), respectively. We see that our approach succeeded in stabilizing the UPO by small control force in spite of a relatively large influence

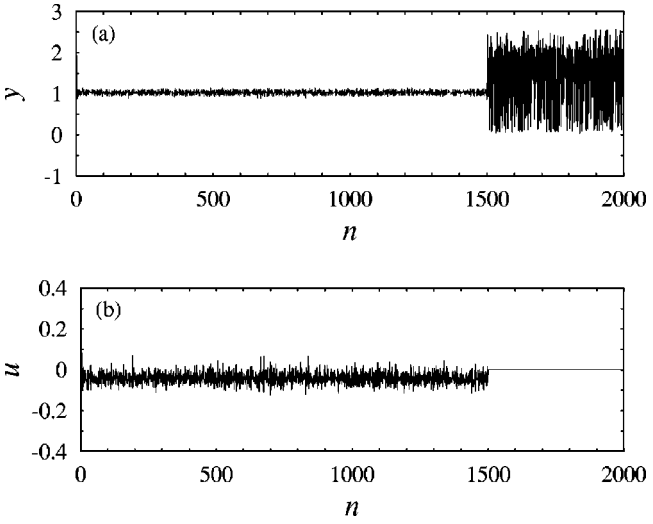

FIG. 5. Result of chaos control for Eqs. (14) with $\kappa=0.6$, $r_2=0.2$, $\delta=0.5$, $\gamma=1.6$, and $\omega=\pi/5$: (a) time series of the dimensionless velocity y sampled at $\omega t=0 \bmod 2\pi$; (b) external feedback control force u. See the text for further information.

of noise. The nonzero feedback control force was required while the target was stabilized because of the influence of noise as well as an error of the detected UPO. We also add that the use of rather large values of κ failed to control chaos. This is due to the fact that the error of the approximate UPO can be seriously amplified and disturbs the stabilization of the target when κ is large.

IV. EXPERIMENTS FOR FORCED, SINGLE AND COUPLED PENDULA WITH DRY FRICTION

We next present experimental results for periodically forced, single and coupled pendula. The experimental system is shown in Fig. 6. Each of the pendula consisted of a brass rod 120 mm long with a 10-mm circular cross section, and a brass disk of 36-mm diameter and 16-mm thickness having a 5-mm-diam hole. They were attached to the shafts of servomotors through the holes. The natural angular frequencies of the pendula about the hanging-down position were estimated as 10.0 rad/s. The velocities of the pendula, $\dot{\theta}_j$, $j=1,2$, were measured from the voltage outputs of generators, and were sampled by a personal computer through electric circuits and an A/D converter at every 1 ms. Each of the servomotors was powered by periodic voltage $V_j(t)=V_{j0}\cos\Omega t$, $j=1,2$. For the coupled pendula case, voltage $\kappa_a(\dot{\theta}_2-\dot{\theta}_1)$ or $\kappa_a(\dot{\theta}_1-\dot{\theta}_2)$ was also supplied to the servomotor, where κ_a is a constant. It was difficult to find UPOs from time series of the velocities when damping is small. So voltage $-\kappa_d\dot{\theta}_j$, $j=1,2$, with κ_d a constant was added to increase the actual damping constants. These input signals were computed on a personal computer and output through a D/A converter. The output signals of the generators and input signals of the servomotors were also monitored with a digital oscilloscope.

The servomotors used in the experiments had a damping characteristic of a dry friction type. So the dimensionless equations of motion are approximately given by

$$\dot{x}_1=x_2,$$
$$\dot{x}_2=-\sin x_1-\delta_1 x_2-\delta_0\,\mathrm{sgn}\,x_2+\gamma\cos\omega t \tag{15}$$

for the single pendulum, and

$$\dot{x}_1=x_2,$$
$$\dot{x}_2=-\sin x_1-\delta_1 x_2-\delta_0\,\mathrm{sgn}\,x_2+\gamma_1\cos\omega t-\alpha(x_2-x_4),$$
$$\dot{x}_3=x_4, \tag{16}$$
$$\dot{x}_4=-\sin x_3-\delta_1 x_4-\delta_0\,\mathrm{sgn}\,x_4+\gamma_2\cos\omega t-\alpha(x_4-x_2)$$

for the coupled pendula, where δ_1, δ_0, γ, γ_1, γ_2, ω, and α are constants and sgn represents the signum function. The outputs for the single and coupled pendula are $y=x_2$ and $y=(y_1,y_2)^T=(x_2,x_4)^T$, respectively, with T the transpose operator. The constants δ_1 and δ_0 were experimentally estimated as $\delta_1=0.39$ and $\delta_0=0.14$. More details on the experimental system are given elsewhere [20]. Henceforth we set the other parameter values as $\gamma=1.25$ and $\omega=0.7$ for the single pendulum, and as $\gamma_1=1.4$, $\gamma_2=0.5$, $\omega=0.7$, and $\alpha=0.3$ for the coupled pendula.

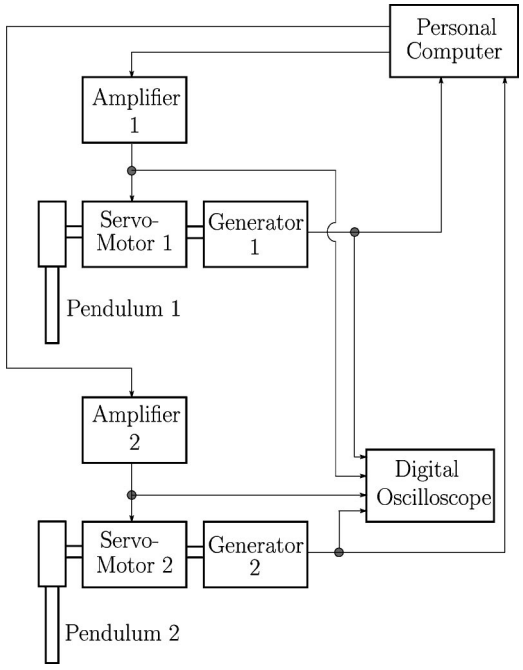

FIG. 6. Block diagram of the experimental apparatus.

Figure 7 shows chaotic attractors obtained experimentally and numerically for the single and coupled pendula.[2] In Figs. 7(a) and 7(b), the delay coordinates are used. Two- and four-dimensional coordinates are enough for our purpose in the single and coupled pendula, respectively (see Sec. III and the Appendix), although the attractors in Figs. 7(a) and 7(b) are obviously folded. In numerical simulations of Figs. 7(b) and 7(d), Gaussian white noises with intensity $\sigma=0.03$ were added in the second equation of Eqs. (15) and in the second and fourth equations of Eqs. (16). Agreements between the experimental and numerical chaotic attractors are fine. We suspect that small differences result from the occurrence of stick motions of the pendula in experiments due to damping characteristics of a dry friction type as well as errors of the estimated parameter values.

The approach of Sec. II with $(r_0,r_1)=(0.03,0.1)$ and $(r_{01},r_{02},r_{11},r_{12})=(0.03,0.03,0.3,0.1)$ was applied to obtain approximate τ-periodic orbits $\tilde{y}(t)$ for the single pendulum and $(\tilde{y}_1(t),\tilde{y}_2(t))$ for the coupled pendula. Here r_{0j} and r_{1j}, respectively, represent the values of r_0 and r_1 in Eqs. (7) and (9) for the jth pendulum, $j=1,2$. The successive points were regarded as approximate loci of τ-periodic orbits or as the target UPOs only if condition (7) or (9) holds for both pen-

[2]We used the computer software DYNAMICS [14] to compute the Lyapunov exponents for Eqs. (15) and (16) with the approximate sgn function (17). Only one positive Lyapunov exponent was obtained for both cases and approximately estimated as 0.163 for Eqs. (15) and 0.0869 for Eqs. (16).

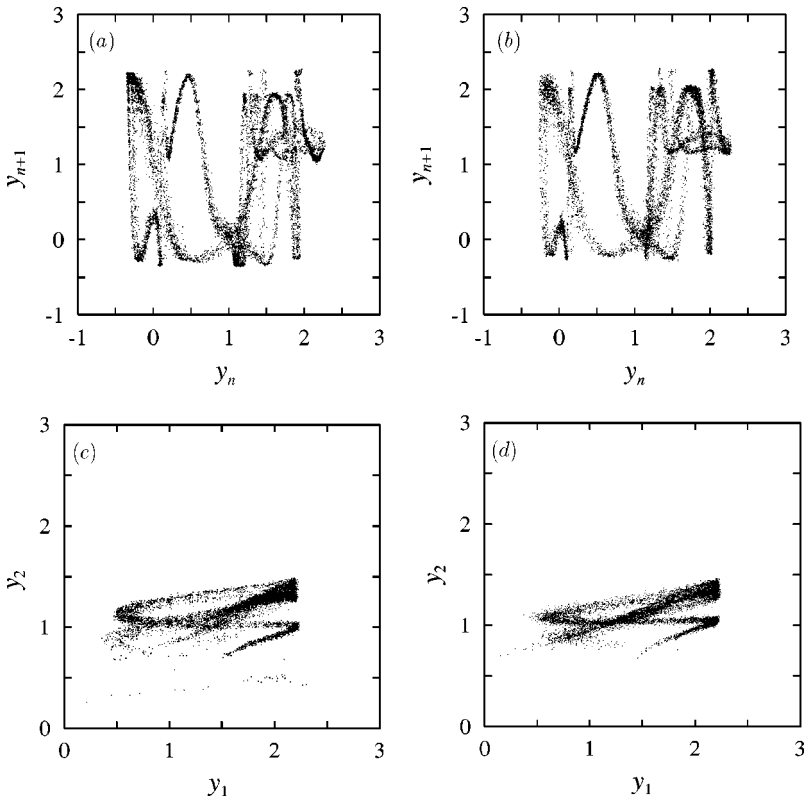

FIG. 7. Experimentally and numerically observed chaotic attractors: (a) and (b) experimental and numerical results for the single pendulum; (c) and (d) experimental and numerical results for the coupled pendula. In numerical simulations, Gaussian white noises with intensity $\sigma=0.03$ are added.

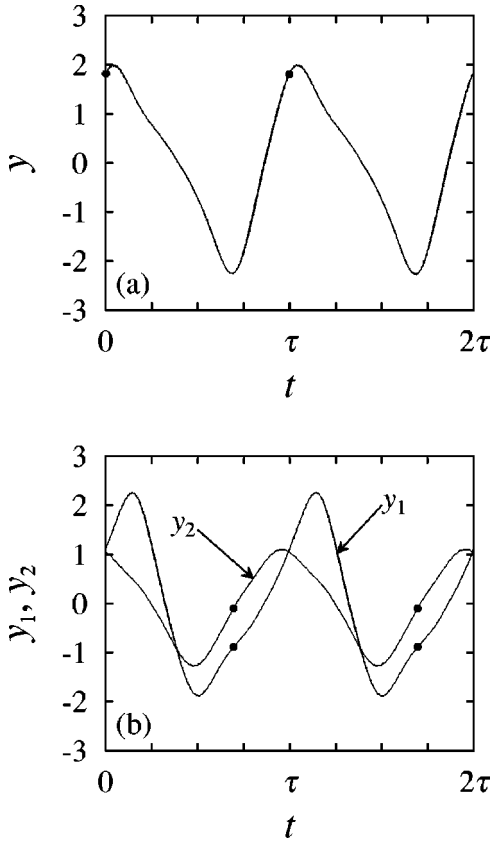

FIG. 8. Approximate UPOs found in experiments: (a) single pendulum; (b) coupled pendula. The dots represent an edge of the UPOs.

dula. The obtained, approximate UPOs are shown in Fig. 8. In these cases, other UPOs could be detected except symmetric counterparts.

To stabilize the UPOs of Fig. 8, we apply the external feedback control such that control force $u=\kappa(\tilde{y}(t)-y)$ and $u_j=\kappa_j(\tilde{y}_j(t)-y_j)$, $j=1,2$, was supplied to each of the pendula for the single and coupled pendula, respectively. Again, using the computer software AUTO with the driver HomMap, we computed the stability boundaries for numerically computed UPOs corresponding to the approximate UPOs of Fig. 8. In the computations, the sgn function was approximated as

$$\operatorname{sgn}\zeta \approx \frac{2}{\pi}\arctan(a\zeta) \tag{17}$$

with $a=50$. The computed stability boundaries are shown in Fig. 9. In Fig. 9(a), the periodic force amplitude γ is varied, and the stability boundaries when the delayed feedback control $\kappa(y(t-\tau)-y(t))$ is applied instead of the external feedback control are also drawn. We see that the stability regions for the UPOs are rather wide. In particular, for the coupled pendula, the UPO can be stabilized by applying control force to only one of the pendula.

Figures 10 and 11 show the experimental results for the single and coupled pendula, respectively. Here $\kappa=0.5$ and $r_2=0.2$ for the single pendulum in Fig. 10, and $\kappa_1=0.6$, $\kappa_2=0$, and $r_{21}=r_{22}=0.2$ for the coupled pendula in Fig. 11, where r_{2j} represents the value of r_2 in (13) for the jth pendulum, $j=1,2$. Only when condition (13) holds for both pendula was the control force applied. The dimensionless pendulum velocities and control force at $\omega t=0 \mod 2\pi$ are plotted. Attempts to stabilize the UPOs from $n=0$ to n

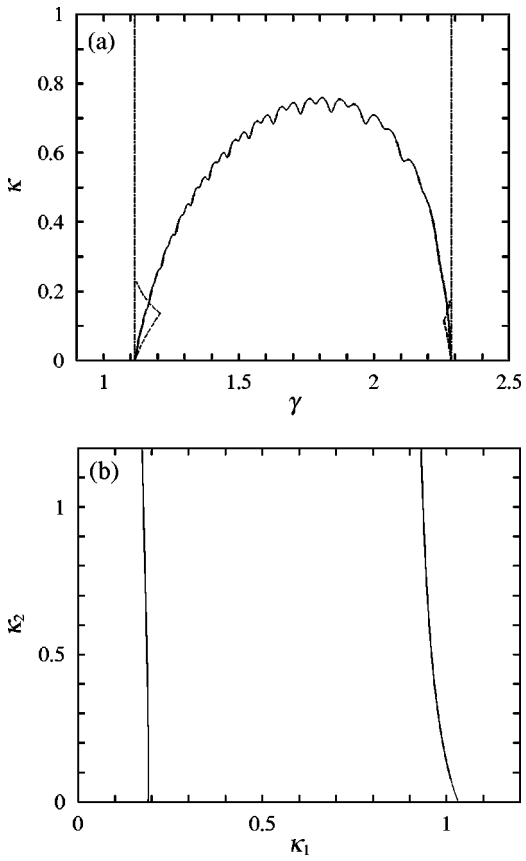

FIG. 9. Stability boundaries of accurate UPOs in Eqs. (15) and (16) with the approximate sgn function of Eq. (17): (a) single pendulum; (b) coupled pendula. The UPOs correspond to the approximate UPOs in Figs. 8(a) and 8(b). The solid curves represent the stability boundaries for the UPOs when the external feedback control is applied. The UPOs become stable above the curve in (a) and between the curves in (b). Also, in (a), the broken and dash-dotted curves, respectively, represent the stability boundaries when the delayed feedback control and no control are applied.

$=1500$ were made and no control force was applied after $n=1500$. We see that our approach succeeded in stabilizing the target UPOs in spite of relatively large influences of noise, again. It should also be noted that the control force was applied to only one pendulum for the coupled pendula.

V. CONCLUSIONS

In this paper, we have applied the external feedback technique to control chaos using approximate UPOs obtained from chaotic times series. We demonstrated its usefulness and effectiveness for periodically forced, single and coupled pendula in numerical simulations and experiments. In particular, our approach succeeded in controlling chaos in actual experiments under relatively large influence of noise. Moreover, in our examples, it could stabilize the target in wide parameter regions, while the delayed feedback technique could only do so in very narrow ones. Thus, we showed that the external feedback technique is as promising in chaos control of continuous systems as the delayed feedback technique.

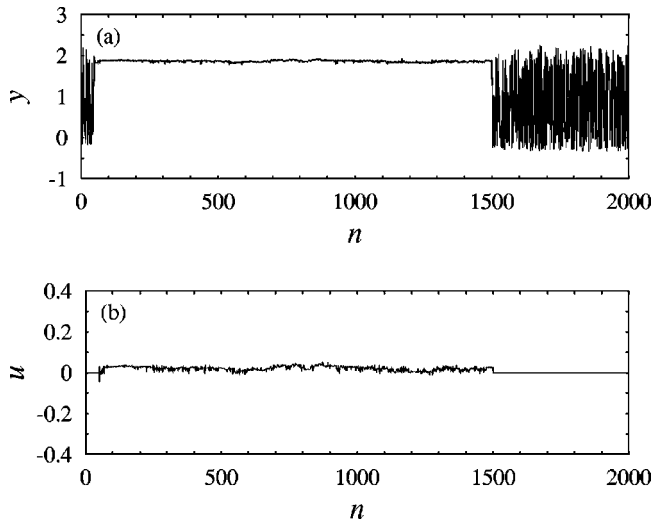

FIG. 10. Result of chaos control for the single pendulum with $\kappa=0.5$ and $r_2=0.2$: (a) time series of the dimensionless velocity y sampled at $\omega t=0$ mod 2π; (b) external feedback control force u. See the text for further information.

Finally, we give some comments on further work to improve our results. First, it is often difficult to precisely detect UPOs from chaotic time series by the technique of [11]. The imprecision of the UPOs yields a problem in our approach of

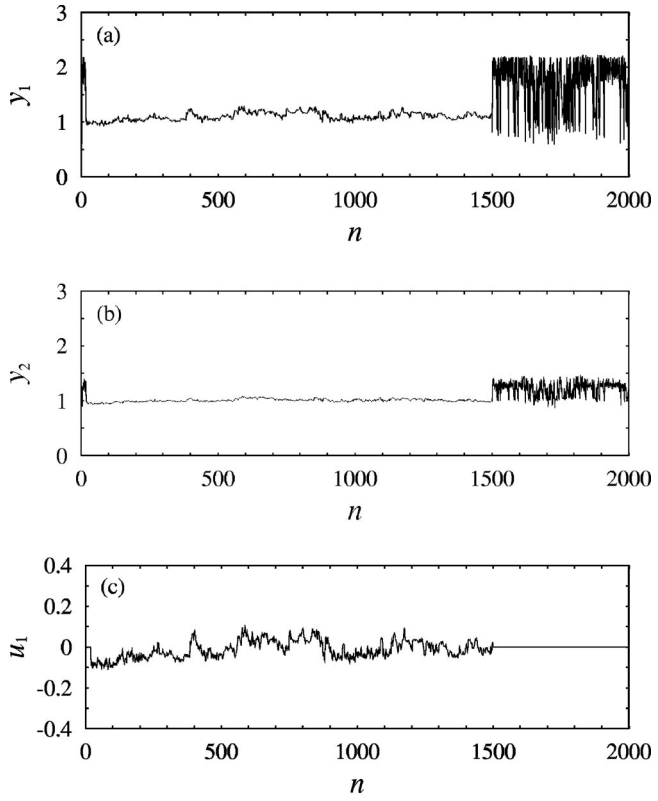

FIG. 11. Result of chaos control for the coupled pendula with $\kappa_1=0.6$, $\kappa_2=0$, and $r_{21}=r_{22}=0.2$: (a) and (b) time series of the dimensionless velocities y_1 and y_2 sampled at $\omega t=0$ mod 2π; (c) external feedback control force u_1. See the text for further information.

controlling chaos especially when nonsmall feedback gain is required since large control force has to be applied. Moreover, when they have too strong unstable directions, the UPOs are difficult to find. It is desired to resolve these difficulties. The method of [21] may be helpful to this end.

Second, in our examples, the governing equations were *a priori* known at least approximately, so that the feedback gain could be estimated. However, in many applications the governing equations are unknown and such an estimation of the feedback gain is not given. So a method of determining the feedback gain from chaotic time series is expected to be developed. Some work has been progressing in these directions and will be reported elsewhere.

ACKNOWLEDGMENT

One of the authors (K. Y.) was partially supported by a Grant-in-Aid for Scientific Research from the Japan Society for the Promotion of Science, 10650236.

APPENDIX: RELATIONSHIP BETWEEN ORIGINAL AND DELAY COORDINATES

Consider a two-dimensional discrete dynamical system

$$(u_{n+1},v_{n+1})=(\varphi(u_n,v_n),\psi(u_n,v_n)). \tag{A1}$$

We want to transform this system from the original coordinates (u_n,v_n) to delay coordinates (u_{n-1},u_n). Another choice of (v_{n-1},v_n) can be treated similarly.

Suppose that

$$\frac{\partial\varphi}{\partial v}(\overline{u}_{n-1},\overline{v}_{n-1})\neq 0 \tag{A2}$$

for some point $(\overline{u}_{n-1},\overline{v}_{n-1})$. Let $\overline{u}_n=\varphi(\overline{u}_{n-1},\overline{v}_{n-1})$. Then we apply the implicit function theorem to

$$u_n=\varphi(u_{n-1},v_{n-1}) \tag{A3}$$

near $(u_{n-1},v_{n-1})=(\overline{u}_{n-1},\overline{v}_{n-1})$ to show that there is a function $h:\mathbb{R}^2\to\mathbb{R}$ such that $\overline{v}_{n-1}=h(\overline{u}_{n-1},\overline{u}_n)$ and $v_{n-1}=h(u_{n-1},u_n)$ satisfies Eq. (A3) for any (u_{n-1},u_n) near $(\overline{u}_{n-1},\overline{u}_n)$. Hence, since $v_n=\psi(u_{n-1},v_{n-1})$,

$$u_{n+1}=\varphi(u_n,\psi(u_{n-1},h(u_{n-1},u_n))) \tag{A4}$$

near $(\overline{u}_{n-1},\overline{u}_n)$. Thus we can rewrite the system (A1) in the two-dimensional delay coordinates (u_{n-1},u_n) near the point $(\overline{u}_{n-1},\overline{u}_n)$. In particular, if an attractor of Eq. (A1) includes $(\overline{u}_{n-1},\overline{u}_n)$, then the local dimension of the attractor at that point is at most 2. Note that condition (A2) holds at almost all points in a general setting.

It can also be proved analogously for higher-dimensional systems that the number of delay coordinates locally required is generally at most the same as that of the original coordinates.

[1] G. Chen and X. Dong, *From Chaos to Order: Methodologies, Perspectives and Applications* (World Scientific, Singapore, 1998).

[2] *Handbook of Chaos Control*, edited by H. G. Schuster (Wiley-VCH, New York, 1999); S. Boccaletti, C. Grebogi, Y.-C. Lai, H. Mancini, and D. Maza, Phys. Rep. **329**, 103 (2000).

[3] K. Pyragas, Phys. Lett. A **170**, 421 (1992).

[4] W. Just, E. Reibold, and H. Benner, in *The 5th Experimental Chaos Conference*, edited by M. Ding, W. L. Ditto, L. M. Pecora, and M. L. Spano (World Scientific, Singapore, in press).

[5] J. E. S. Socolar, D. W. Sukow, and D. J. Gauthier, Phys. Rev. E **50**, 3245 (1994); S. Boccaletti and F. T. Arecchi, Physica D **96**, 9 (1996); W. Just, *ibid.* **142**, 153 (2000).

[6] M. E. Bleich and J. E. S. Socolar, Phys. Lett. A **210**, 87 (1996).

[7] H. Nakajima, Phys. Lett. A **232**, 207 (1997); H. Nakajima and Y. Ueda, Physica D **111**, 207 (1998).

[8] N. F. Rulkov, L. S. Tsimring, and H. D. I. Abarbanel, Phys. Rev. E **50**, 314 (1994).

[9] G. Chen and X. Dong, Int. J. Bifurcation Chaos Appl. Sci. Eng. **3**, 1363 (1993).

[10] N. H. Packard, J. P. Crutchfield, J. D. Farmer, and R. S. Shaw, Phys. Rev. Lett. **45**, 712 (1980); T. Takens, in *Dynamical Systems and Turbulence, Warwick, 1980*, edited by D. A. Rand and L.-S. Young, Lecture Notes in Math. Vol. 898 (Springer, New York, 1981); J. D. Farmer and J. J. Sidorowich, Phys. Rev. Lett. **59**, 845 (1987).

[11] D. P. Lathrop and E. J. Kostelich, Phys. Rev. A **40**, 4028 (1989).

[12] H. Nijmeijer and A. J. van der Schaft, *Nonlinear Dynamical Control Systems* (Springer, New York, 1990).

[13] K. Yagasaki and Y. Tochio, Int. J. Bifurcation Chaos (to be published).

[14] H. E. Nusse and J. A. Yorke, *Dynamics: Numerical Explorations*, 2nd ed. (Springer, New York, 1997).

[15] H. D. I. Abarbanel, *Analysis of Observed Chaotic Data* (Springer, New York, 1996).

[16] E. Doedel, A. R. Champneys, T. F. Fairgrieve, Y. A. Kuznetsov, B. Sandstede, and X. Wang, AUTO97: *Continuation and Bifurcation Software for Ordinary Differential Equations (with HomCont)* (Concordia University, Montreal, 1997).

[17] K. Yagasaki, Int. J. Bifurcation Chaos Appl. Sci. Eng. **7**, 1617 (1998); K. Yagasaki, *HomMap: An AUTO Driver for Homoclinic Bifurcation Analysis of Maps and Periodically Forced Systems* (Gifu University, Gifu, Japan, 1998).

[18] J. Hale and S. M. V. Lunel, *Introduction to Functional Differential Equations* (Springer, New York, 1993).

[19] W. Just, T. Bernard, M. Ostheimer, E. Reibold, and H. Benner, Phys. Rev. Lett. **78**, 203 (1997); W. Just, E. Reibold, K. Kacperski, P. Fronczak, J. A. Holyst, and H. Benner, Phys. Rev. E **61**, 5045 (2000).

[20] K. Yagasaki (unpublished).

[21] P. So, E. Ott, S. J. Schiff, D. T. Kaplan, T. Sauer, and C. Grebogi, Phys. Rev. Lett. **76**, 4705 (1996); P. So, E. Ott, T. Sauer, B. J. Gluckman, C. Grebogi, and S. J. Schiff, Phys. Rev. E **55**, 5398 (1997).